original article

Annals of Oncology 20: 1943–1947, 2009
doi:10.1093/annonc/mdp242
Published online 1 July 2009

Phase I/II clinical study of percutaneous vertebroplasty (PVP) as palliation for painful malignant vertebral compression fractures (PMVCF): JIVROSG-0202

T. Kobayashi[1]*, Y. Arai[2], Y. Takeuchi[2], Y. Nakajima[3], Y. Shioyama[4], M. Sone[5], N. Tanigawa[6], O. Matsui[7], M. Kadoya[8] & Y. Inaba[9] Japan Interventional Radiology in Oncology Study Group (JIVROSG)

[1]*Department of Diagnostic and Interventional Radiology, Ishikawa Prefectual Central Hospital, Ishikawa;* [2]*Department of Diagnostic Radiology Division, National Cancer Center Hospital, Tokyo;* [3]*Department of Radiology, St. Marianna University, Yokohama;* [4]*Department of Radiology, Dokkyo Medical University, Tochigi;* [5]*Department of Radiology, Iwate Medical University, Iwate;* [6]*Department of Radiology, Kansai Medical University, Isaka;* [7]*Department of Radiology, Kanazawa University, Ishikawa;* [8]*Department of Radiology, Shinshu University, Matsumoto and* [9]*Department of Diagnostic and Interventional Radiology, Aichi Cancer Center, Aichi, Japan*

Received 8 May 2008; revised 18 November 2008; revised 18 March 2009; accepted 26 March 2009

Background: The safety and efficacy of percutaneous vertebroplasty (PVP), a new treatment modality for painful malignant vertebral compression fractures (PMVCF) using interventional radiology techniques, were evaluated prospectively.
Materials and methods: After confirming the absence of safety issues in phase 1, a total of 33 cases were registered up to and including phase 2. Safety and efficacy were evaluated by National Cancer Institute—Common Toxicity Criteria version 2 and Visual Analogue Scale (VAS) at 1 week after PVP. Based on VAS score decreases, efficacy was classified into significantly effective (SE; ≥5 or reached 0–2), moderately effective (ME; 2–4), or ineffective (NE; <2 or increase).
Results: Procedures were completed in all 33 patients (42 vertebrae). Thirty days after PVP, two patients died of primary disease progression, but no major adverse reactions (>grade 2) were observed. Response rate was 70% (95% confidence interval 54% to 83%) [61% (n = 20) with SE, 9% (n = 3) with ME, and 30% (n = 10) with NE] and increased to 83% at week 4. Median time to response was 1 day (mean 2.4). Median pain-mitigated survival period was 73 days.
Conclusion: For PMVCF, PVP is a safe and effective treatment modality with immediate onset of action.
Key words: percutaneous vertebroplasty, interventional radiology, pain relief, vertebral metastasis, percutaneous cement plasty

introduction

The pain relief of painful malignant vertebral compression fractures (PMVCF) is one of the key elements for achieving better quality of life in patients under palliative care. The mainstay for pain relief is pharmacological therapy such as with nonsteroidal anti-inflammatory drugs (NSAIDs) and opioids, and if patients are not responsive to these agents or have pain upon body movement, radiotherapy is administered. However, despite being a noninvasive therapeutic modality, radiotherapy is less than ideal because it requires 2–4 weeks to obtain a therapeutic effect and does not achieve complete pain relief in most cases [1, 2].

Since the report of percutaneous vertebroplasty (PVP) by Galibert et al. [3], in 1987, the technique has been widely reported [4–10]. These reports indicate that it is highly effective for prompt pain relief for metastatic vertebral tumors from any primary sites. On the other hand, severe, albeit rare, complications such as pulmonary embolism, cerebral infarction, cardiogenic shock, and spinal cord injury due to leakage of cement into the spinal canal have also been documented [11–13]. All these reports, however, have been retrospective in nature, and to our knowledge, no study has yet prospectively investigated the safety and therapeutic effect of this modality. Although it cannot be excluded that severe complications may very rarely occur, to minimize the frequency of reported complications, it is important to evaluate in a prospective study whether this procedure can be carried out safely when conducted by trained interventional radiologists for clearly defined indications.

Therefore, we undertook a phase I/II multi-institutional prospective study of PVP as Japan Interventional Radiology in Oncology Study Group (JIVROSG)-0202. In this study, we evaluated the safety and efficacy of PVP as a palliative intervention for patients with PMVCF.

materials and methods

patient selection

Patients were required to have an imaging [including radiography and computed tomography (CT)] diagnosis of changes in the thoracic or

*Correspondence to: Dr T. Kobayashi, Department of Diagnostic and Interventional Radiology, Ishikawa Prefectual Central Hospital, Kuratsukihigashi 2-1, Kanazawa-shi, Ishikawa Prefecture, 920-8530, Japan. Tel: +81-76-237-8211; Fax: +81-76-238-2337; E-mail: kobaken@ipch.jp

lumbar vertebrae caused by malignant tumor metastases or multiple myeloma, limitation of daily activities due to pain from the lesions and/or the risk of compression fracture, and no exposure of the vertebral tumors to the vertebral canal (defined as vertebral canal surface showing no tumor invasion on CT or magnetic resonance imaging). In addition, the patients had to have an Eastern Cooperative Oncology Group performance status (PS) of zero to three, preserved major organ function (bone marrow, heart, liver, lung, and kidney), and an anticipated survival of at least 4 weeks. Patients were excluded if their pain grade of Visual Analogue Scale (VAS) [14] was ≤2, they could not maintain the position needed for treatment, they had a bleeding tendency with bleeding time ≥5 min, fever ≥38°C, cardiac failure requiring continuous drug therapy, history of major drug allergy such as anaphylactic shock to any drugs, so as to minimize the possibility of cardiac toxicity due to the bone cement preparation, and/or confirmed or possible pregnancy. In addition, patients were judged ineligible for this trial if the vertebral lesions harbored possible active inflammation (tuberculous or other infectious), if marked vertebral flattening was present (defined as the height of the affected vertebral body showing a mean value of one-third of that of the superior and inferior vertebral bodies), if five or more continuous vertebrae were affected precluding evaluation of the therapeutic effect or if in a single session four or more vertebrae required therapy.

Both the ethics committee of the Japanese Society of Interventional Radiology and each institutional review board approved the protocol of this study before patient entry. All patients provided written informed consent.

collaborative institutions

This study was conducted in 10 institutions comprising JIVROSG. Each of these institutions has at least one full-time interventional radiologist certified by the Japanese Society of Interventional Radiology (Table 1).

study end points

The primary end point of this study was to evaluate the safety of PVP, and the secondary end point was to evaluate the efficacy of PVP for pain relief as well as the incidence and grade of adverse events.

study design

This study was a multi-institutional, single-arm, open-label, noncomparative trial. The phase I part of this trial was conducted using the 3 × 3 method proposed by the JIVROSG. This method was applied as follows. To be able to quickly terminate the study if the incidence of adverse events associated with this modality exceeded one-third of the patients, three separate groups with three cases each were enrolled at 4-week intervals. If severe adverse events of the first group with three cases, according to the National Cancer Institute—Common Toxicity Criteria (NCI-CTC) version 2.0 [15] or equivalent adverse events, were limited to one or less of the first three cases, then the second group with three cases was added. When the number of adverse events in the combined first and second groups with six cases was two or less, then the third group with three cases was added. If the number of adverse events of the total nine cases of all three groups was three or less, then subsequently all cases up to the target number were enrolled without distinguishing them into three different groups. If the incidence of adverse events in each of the first, second and third groups exceeded the above-noted permissible limits, the advisability of trial continuation or possible termination was rediscussed.

Table 1. Collaborative institutions

National Cancer Center Hospital
Kyoto First Red Cross Hospital
St Marianna University
Ibaraki Prefectural Central Hospital
Kansai Medical University
Iwate Medical University
Kanazawa University
Shinshu University
Aichi Cancer Center
Tochigi Cancer Center Hospital

In the phase II part of this study, 24 cases were enrolled. Since the treatment administered in phases 1 and 2 was exactly the same, the primary and secondary end points of the cases registered in phase 1 were evaluated together with those of the cases of phase 2. So, the primary and secondary end points were evaluated in all 33 cases.

The observation period for adverse events was defined as the 1-month period following the completion of the procedure. Subsequently, the presence/absence of pain recurrence at the treated site, the period of pain relief (absence of recurrent pain at the treated site from before therapy to obtaining a decrease of VAS score to ≤2), and patient survival period were investigated. In the follow-up investigation, recurrence was defined as occurring on the day on which pain worse than that before therapy was noted, with the period up to this day defined as the pain-mitigated survival period.

statistical analysis

In the phase I part of this study, a cohort size of nine patients was considered to make it possible to quickly terminate the study if the incidence of adverse events associated with this modality exceeded one-third. During phase I through phase II, the study was designed to detect adverse events having an incidence of at least 10%, setting 80% power, 10% predicted rate, and 30% unacceptable rate. We anticipated a protocol dropout rate of 10%. Thus, the target accrual number of patients was calculated to be 33. All enrolled patients were included for the intention-to-treat analyses.

registration of cases

The registration period extended from February 2003 until May 2006. To enter a patient into the study, the investigator had to log on to a restricted Web site using the JIVROSG data center, enter patient indication/contraindication data, and register the case. After the executive office verified the suitability of the entered data and the presence/absence of any missing items, a registration number specific to that patient was issued and the case registration procedure completed. Subsequently, all communications were limited to these issued patient registration numbers. PVP was commenced within 1 week of this patient registration.

interventional procedures of PVP

The interventional procedures of PVP in this study were conducted as follows. After injection of 0.5 mg atropine sulfate and securing a venous access, the patient was placed prone on the table used for fluoroscopy or CT fluoroscopy, and an electrocardiogram apparatus and blood pressure monitor were attached. Following disinfection of the puncture site and injection of local anesthesia, an 11–14 ga metallic needle was inserted up to the site where the bone cement was to be injected under fluoroscopic or CT-fluoroscopic guidance (Figure 1A). Acrylic bone cement was prepared, and the use of bone cement mixed with up to 30% bactericidal barium was recommended if bone cement was injected under fluoroscopic guidance (Figure 1B). The injection was stopped when sufficient bone cement was judged to have been distributed, after which the needle was withdrawn (Figure 1C). When multiple (up to three) vertebrae were to be treated, these steps were repeated for each vertebra. The patient was kept at bed rest for 2 h after the procedure.

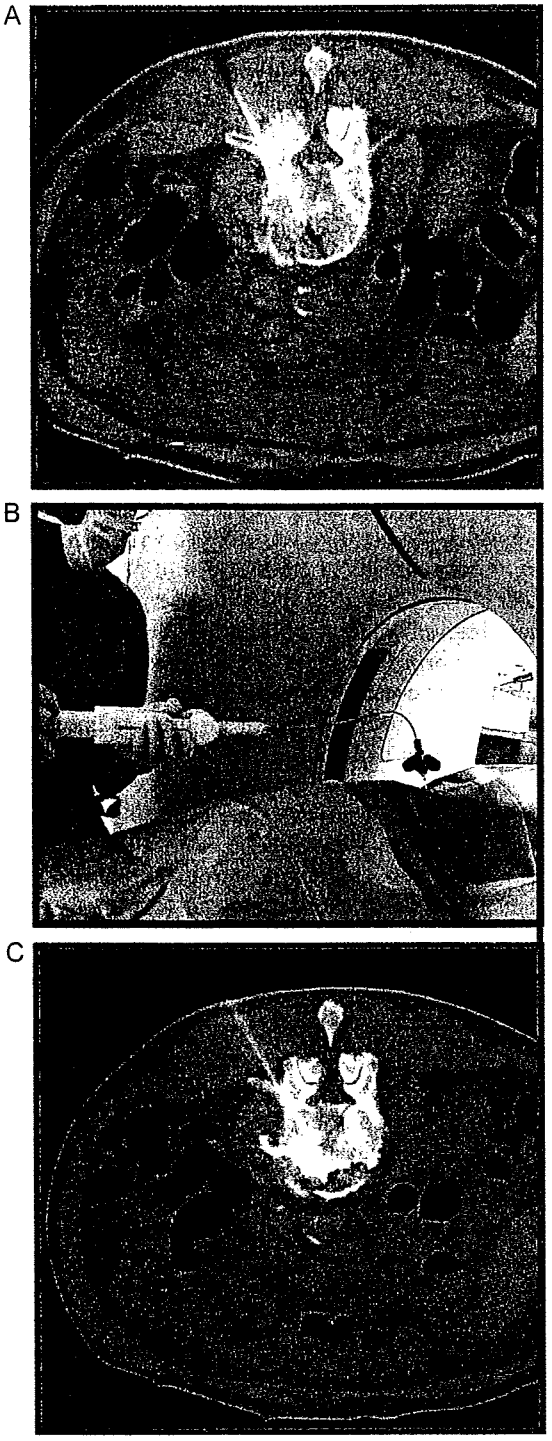

Figure 1. Interventional procedure of percutaneous vertebroplasty. (A) Insertion of 11–14 ga bone biopsy needle into the target vertebral bone through pedicle under fluoroscopic or computed tomography (CT)-fluoroscopic guidance. (B) Injection of acrylic bone cement under fluoroscopy or CT fluoroscopy monitoring. (C) Stop of the injection when adequate distribution is obtained.

combined and supportive therapies

To prevent possible infection, it is recommended that antibiotics be administered for 3 days following the procedure and that an anesthesiologist or other physician able to undertake emergency measures be present. Continued administration of any radiotherapy or analgesics, chemotherapy, and nerve block therapy used before therapy was permitted, including the wearing of corsets. With the exception of management of adverse events, surgical intervention for post-therapy pain, admixture of anticancer agents and/or antibiotics with the acrylic bone cement, and PVP using general anesthesia were not permitted.

observation items

The imaging findings including those of radiography and CT of the primary site and target vertebrae and compression grade were evaluated before therapy and at around 7 days after therapy. VAS score was determined at days 1, 3, and 7 and weeks 2 and 4. Also, before and after therapy, the patient items were evaluated at the specified times.

evaluation methods

The adverse events were evaluated by NCI-CTC version 2. The grade of pain was evaluated by the VAS. VAS scoring was done by having the patient himself note his degree of pain on a 10-cm long horizontal straight line. The efficacy of therapy was evaluated by changes in the VAS score noted 1 week after therapy. When the VAS score was ≤2 or when compared with before therapy a decrease of ≥5 was obtained, the therapy was judged to be significantly effective (SE). When the VAS score did not reach ≤2 but when compared with before therapy showed a decrease to <5 to ≥2, the therapy was judged to be moderately effective (ME). When despite therapy the VAS score decreased by <2 or showed an increase, the therapy was judged to be ineffective (NE). The efficacy of the therapeutic results was assessed by the proportion of the total cases achieving SE or ME. Regardless of any changes in the VAS score, the therapy was also judged to be NE if the need for analgesics increased as compared with before therapy. However, to investigate the timing of the pain-mitigating effect, VAS score was determined within 1 week before the start of therapy, the day after, 3 days after, and at 1, 2, 3, and 4 weeks.

In cases with painful bone metastases at multiple sites, treatment was permitted for all sites with indications for PVP at multiple sessions. However, one treatment session was limited to a maximum of three vertebrae. When all treatment sessions were finished, the degree of back pain was comprehensively evaluated by VAS.

results

There were no reports of severe adverse event in any of the nine cases enrolled in phase I. Thus, without any interruption the transition was made to phase II. There were a total of 33 cases from 10 institutions, comprising 16 males and 17 females with a mean age of 62 years (37–87 years) (Table 2). PS was zero in one case, one in seven cases, two in 12 cases, and three in 13 cases. Thirty cases had metastatic vertebral tumors, originating from lung, breast, and colon cancer in seven cases each, liver cancer in four cases, pancreas cancer in two cases, and tongue, esophagus, and skin cancer in one case each. The only primary vertebral tumor was multiple myeloma, which was present in three cases. Analgesics administered before therapy were NSAIDs alone in nine cases, opioids alone in 10, and both in 11. Radiotherapy was administered to the treated site in 11 cases. The mean interval between the two therapies was 46 days, and no pain-mitigating effect was obtained.

Forty-two vertebrae were targeted: 18 thoracic vertebrae (I, one; VII, three; VIII, three; IX, four; X, two; XI, two; and XII, three) and 24 lumbar vertebrae (I, one; II, seven; III, seven; IV, seven; and V, two). Changes in imaging findings at the treated sites comprised osteolytic changes in 35 vertebrae, mixed

changes in five vertebrae, and osteoblastic changes in two vertebrae, with the mean compression rate amounting to 75.8% (41%–106%). Three vertebral bodies, two vertebral bodies, and one vertebral body were treated in two, five, and 26 cases, respectively. In only a single case was the treatment divided into two sessions, being completed in a single session in all the other cases.

Table 2. Background of enrolled cases

Patient characteristics	*n*
No. of patients	33[a]
Male	16
Female	17
Mean age, years	62 (37–87)
Primary disease	
Lung cancer	7
Breast cancer	7
Colorectal cancer	7
Liver cancer	4
Myeloma	3
Pancreatic cancer	2
Tongue cancer	1
Esophageal cancer	1
Skin cancer	1
Preradiotherapy to the target lesion	11 (mean interval 46 days)
Combined chemotherapy	16
Administered analgesics before therapy	
NSAIDs alone	9
Opioids alone	10
NSAIDs and opioids	11
Performance status (ECOG)	
0	1
1	7
2	12
3	13
Target VB ($N = 42$)	
1 VB	26
2 VBs	5
3 VBs	2
Thoracic VB ($N = 18$)	
I	1
VII	3
VIII	3
IX	4
X	2
XI	2
XII	3
Lumbar VB ($N = 24$)	
I	1
II	7
III	7
IV	7
V	2
Appearance of lesion	
Osteolytic	28 (35 VBs)
Mixed	3 (5 VBs)
Osteoblastic	2 (2 VBs)
Compression rate (height of target VB/height of next VB)	
Mean	75.8% (41%–106%)

[a]Nine for phase I and 24 for phase II.
NSAIDs, nonsteroidal anti-inflammatory drugs; ECOG, Eastern Cooperative Oncology Group; VB, vertebral bone.

CT fluoroscopy was used in 15 cases, fluoroscopy in 15, and a combination of the two in three. The mean time required per case and per vertebra was 49 min (20–120 min) and 39 min, respectively. The volume of bone cement administered was 1–8 ml [mean 3.5 ml, standard deviation (SD) 1.8 ml]. The bone cement preparations used were Osteobond (Zimmer, IN) in 22 cases, Simplex (Stryker, MI) in 10, and Bone Cement (Zimmer) in one. The recommended antibiotics were used in 19 of 33 cases (58%). The technical success rate was 100%, and in no cases were the interventional procedures provided by the protocol terminated prematurely.

In the evaluation of safety, adverse events during the therapy were limited to bleeding from the puncture site in a single case (3%), in which the bleeding was stopped with 5-min manual pressure. Adverse events of grade 3 or 4 of NCI-CTC version 2 or other correspondingly severe adverse events related to PVP were not observed, while two patient deaths caused by the progression of primary disease were observed within 30 days of PVP. An adverse event of PVP could not be excluded in only a single case (3%) with grade 2 serum hypoalbuminemia.

In the evaluation of clinical efficacy, the response rate was 70% (95% confidence interval 54% to 83%), being SE in 20 cases (61%) and ME in three (9%). The mean time to response was 2.4 days (median 1 day, SD 3.2 days). VAS score was 6.2 + 2.1 within 1 week before the start of therapy, 3.6 + 2.6 the day after, 2.5 + 2.6 after 3 days, and 2.4 + 2.3 at 1 week (5–8 days), 2.3 + 2.7 at 2 weeks (11–15 days), 2.0 + 2.2 at 3 weeks (15–26 days), and 1.8 + 2.3 at 4 weeks (26–29 days) (Figure 2).

Pain recurrence at the treated site was noted in 5 of 23 (22%) of the SE or ME cases. On the other hand, in 4 of the 10 cases (40%) in which the therapy was evaluated as ineffective in the first week, the result was subsequently judged to be ME. At 4 months after completion of enrollment, 14 patients were alive, 18 had died, and the survival status of one was unknown. The median survival period was 194 days (mean 270 days, SD 240

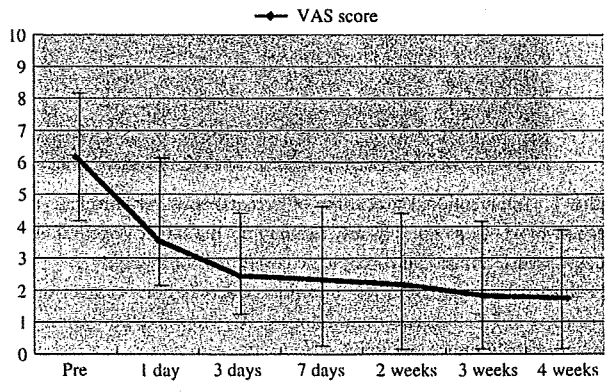

Figure 2. Changes in Visual Analogue Scale (VAS) score. The changes in the VAS values at the various observation time points are listed here. The curve shows the changes in mean values and the vertical line the standard deviation. Pain relief from the therapy is obtained by the third day, with a slow decrease in the VAS values also subsequently observed.

days). The median pain-mitigated survival period was 73 days (mean 230 days, SD 258 days).

discussion

The treatment of painful vertebral metastases and other conditions affecting vertebral bone remains a major challenge in patients under palliative care. Numerous studies have already validated the efficacy and safety of PVP in this context [4–7, 11]. However, all these were retrospective in nature, and no such prospective studies have yet been described. This prompted JIVROSG to undertake the present study to objectively evaluate this procedure by prospectively assessing its safety and clinical efficacy in a multi-institutional setting.

Regarding safety, we attributed the absence of severe complications in the present study to the strict patient selection criteria adopted by us, namely, the exclusion of cases with cardiac failure, a history of drug allergy, and tumors exposed within the vertebral canal, as well as the use of a highly precise fluoroscopy or CT fluoroscopy apparatus at the time of therapy, and the use during fluoroscopy of bone cement mixed with up to 30% bactericidal barium so as to facilitate the immediate recognition of extravertebral leakage. These results indicate that PVP is an extremely safe therapeutic intervention, provided that appropriate patient selection and apparatus use are adhered to, when carried out by an interventional radiology specialist.

In this study, pain was evaluated at 1 week after therapy, with an efficacy rate of 70% obtained, comparable to previously reported results of 70%–90% in the literature [4, 7, 10, 11]. However, most importantly, the therapeutic effect was apparent at a median 1 day (mean 2.4 days, SD 3.2 days), demonstrating a rapid pain-relieving effect. In contrast, the therapeutic response to the hitherto standard pain relief therapeutic modality used, namely, 10 sessions of radiotherapy at 3 Gy, has been reported to require 2–4 weeks to take effect [1, 2]. In this respect, thus, the rapidity of onset of the desired effect of PVP is clearly superior to that of radiotherapy. The median survival period of the enrolled cases was 194 days because ≥90 of them had bone metastases from malignant tumors and had a poor prognosis. In view of this fact, the selection of a therapeutic modality providing a prompt onset of pain relief becomes especially important. In contrast, in cases with vertebral body metastases highly sensitive to radiotherapy and/or with an anticipated long survival period, radiotherapy is the preferred option.

Recurrence of pain at the treated site was noted in 21% of cases. Since this therapy is not designed to exert an antitumor effect but rather to provide pain relief by strengthening weakened vertebrae, pain recurrence is unavoidable if the metastatic foci expand. The lack of a response in six patients was attributed to their poor general state. The present results based on a prospective study demonstrate that PVP can be carried out safely and shows marked efficacy, in particular fast-acting pain relief, provided that patient and equipment selection is appropriate and that an experienced physician is available. Since PVP is a therapeutic technique, its safety cannot be evaluated like that of a phase I trial for drugs in which drug doses are increased incrementally to determine the optimal doses to be administered. Therefore, in the present study, we adopted a modified design of phase I study for drugs. However, the number of cases in our study is not enough to confirm the safety of PVP. Additionally, the results of this study are insufficient to establish PVP as a standard therapy for patients with painful malignant vertebral body tumors. Thus, we are planning to conduct a phase III study comparing PVP and conventional treatments in this context.

conclusion

PVP was proved safe, clinically efficacious, and fast acting in this prospective study. Future studies enrolling larger groups of patients will be needed to further establish its role in the management of painful bone lesions as palliative care.

acknowledgements

This study is the first prospective one to evaluate the safety and efficacy of PVP as palliative care for end-stage cancer patients. The authors have received no funds related to this study and are aware of no conflict of interest. A part of this study was shown as a poster presentation at the meeting of the American Society of Clinical Oncology, Chicago 2007.

references

1. Bates T. A review of local radiotherapy in the treatment of bone metastases and cord compression. Int J Radiat Oncol Biol Phys 1992; 23: 217–221.
2. Ben-Josef E, Shamsa F, Williams O et al. Radiotherapeutic management of osseous metastases: a survey of current patterns of care. Int J Radiat Oncol Biol Phys 1998; 40: 915–921.
3. Deramond H, Depriester C, Galibert P et al. Percutaneous vertebroplasty with polymethylmethacrylate. technique, indication, and results. Radiol Clin North Am 1998; 36: 533–546.
4. Cotton A, Boutry N, Cortet B et al. Percutaneous vertebroplasty: state of the art. Radiographics 1998; 18: 311–320.
5. Barr JD, Barr MS, Lemley TJ et al. Percutaneous vertebroplasty for pain relief and spinal stabilization. Spine 2000; 25: 923–928.
6. Weill A, Chiras J, Simon JM et al. Spinal metastases; indications for and results of percutaneous injection of acrylic surgical cement. Radiology 1996; 199: 241–247.
7. Murphy KJ, Deramond H. Percutaneous vertebroplasty in benign and malignant disease. Neuroimaging Clin N Am 2000; 10: 535–545.
8. Baba K, Ookubo K, Hamada K et al. Percutaneous vertebroplasty for osteolytic metastasis: a case report. Radiat Med 1997; 57: 880–882.
9. Kobayashi T, Takanaka T, Matsui O et al. Efficacy of percutaneous vertebroplasty under CT fluoroscopic guidance. Jpn J Intervent Radiol 1999; 14: 343–348.
10. Kobayashi T, Takanaka T, Matsui O et al. Practice of percutaneous vertebroplasty. Jpn J Intervent Radiol 2002; 17: 17–22.
11. Jensen ME, Kallmes DE. Percutaneous vertebroplasty in the treatment of malignant spine disease. Cancer J 2002; 8: 194–206.
12. Scroop R, Eskridge J, Britz GW. Paradoxical cerebral arterial embolization of cement during intraoperative vertebroplasty: case report. AJNR Am J Neuroradiol 2002; 23: 868–870.
13. Kaaufmann TJ, Jensen ME, Ford G et al. Cardiovascular effects of polymethyl methacrylate use in percutaneous vertebroplasty. AJNR Am J Neuroradiol 2002; 23: 601–604.
14. Wewers ME, Lowe NK. A critical review of visual analogue scales in the measurement of clinical phenomena. Res Nurs Health 1990; 13: 227–236.
15. http://ctep.cancer.gov/protocolDevelopment/electronic_applications/docs/ctcv20_4-30-992.pdf (15 April 2009, date last accessed).

Cardiovasc Intervent Radiol (2009) 32:1059–1066
DOI 10.1007/s00270-009-9510-1

TECHNICAL NOTE

Development of a New Subclavian Arterial Infusion Chemotherapy Method for Locally or Recurrent Advanced Breast Cancer Using an Implanted Catheter–Port System After Redistribution of Arterial Tumor Supply

Kenji Takizawa · Hiroshi Shimamoto · Yukihisa Ogawa · Misako Yoshimatsu · Kunihiro Yagihashi · Yasuo Nakajima · Takashi Kitanosono

Received: 4 August 2008 / Accepted: 8 January 2009 / Published online: 24 February 2009

Abstract Locally or recurrent advanced breast cancers can receive arterial blood supply from various arteries, such as the internal thoracic artery (ITA), the lateral thoracic artery, and the other small arterial branches originating from the subclavian artery. Failure to catheterize and subsequent formation of collateral arterial blood supply from various arteries are some of the reasons why the response to conventional selective transarterial infusion chemotherapy is limited and variable. To overcome this problem, we developed a new subclavian arterial infusion chemotherapy method using an implanted catheter–port system after redistribution of arterial tumor blood supply by embolizing the ITA. We named this technique ("redistributed subclavian arterial infusion chemotherapy" (RESAIC)). Using RESAIC, patients can be treated on an outpatient basis for extended periods of time. Eleven patients underwent RESAIC, and the complete remission and partial response rate in 10 evaluable patients was 90%: complete remission [CR] $n = 4$, partial remission $n = 4$, stable disease $n = 1$, and not evaluable $n = 1$. Three of four patients with CR had no distant metastasis, and modified radical mastectomy was performed 1 month after conclusion of RESAIC. The resected specimens showed no residual cancer cells, and pathologically confirmed complete remission was diagnosed in each of these cases. Although temporary grade-3 myelosuppression was seen in three patients who were previously treated by systemic chemotherapy, there was no other drug-induced toxicity or procedure-related complications. RESAIC produced a better response and showed no major complications compared with other studies despite the advanced stage of the cancers.

Keywords Interventional Radiology · Breast cancer · Arterial infusion chemotherapy · Implanted port

K. Takizawa (✉) · H. Shimamoto · Y. Ogawa · M. Yoshimatsu · K. Yagihashi · Y. Nakajima
Department of Radiology, St. Marianna University School of Medicine, Sugao, Miyamae, Kawasaki, Kanagawa, Japan
e-mail: taki-lrl@vy.catv.ne.jp

H. Shimamoto
e-mail: hshima@k8.dion.ne.jp

Y. Ogawa
e-mail: yukky-p406c@nifty.com

M. Yoshimatsu
e-mail: misako_yosh@yahoo.co.jp

K. Yagihashi
e-mail: yagiku@hotmail.com

Y. Nakajima
e-mail: y3naka@marianna-u.ac.jp

T. Kitanosono
Department of Vascular/Interventional Radiology, University of Rochester Medical Center, 601 Elmwood Avenue, Box 648, Rochester, NY, USA
e-mail: tkita1@mac.com

Introduction

Locally or recurrent advanced breast cancers (ABC) are defined as large tumors with extensive regional lymph node involvement or direct invasion of the skin or underlying chest wall [1]. These cancers are considered stages IIIa and IIIb according to the tumor-node-metastasis classification system adopted by the Japanese Breast Cancer Society, which is based on the classification system of the International Union Against Cancer [2]. Inflammatory breast cancer showing extensive histologic infiltration of dermal lymphatics is a distinct subset.

Some previous reports showed that arterial infusion chemotherapy (AIC) was effective for ABC [3–5]. The local response rate was reported to be 70–90%, and rapid tumor regression was seen after the treatment [6–10]. However, problems associated with AIC should be resolved as will be described later. Conventionally in AIC procedures, the chemotherapeutic agents are selectively infused into subclavian and axillary branches supplying the tumor. This procedure is technically complicated and is usually repeated multiple times in each patient. In addition, such repeated infusions cause drug-induced damage to the infused arterial branches, and this promotes the development of collateral arterial blood supply [11, 12]. Therefore, the number of possible repetitions of AIC is limited, and long-term local control is not expected. To overcome this problem, we developed a new subclavian arterial infusion chemotherapy method using an implanted catheter–port system (CPS) after redistribution of the arterial blood supply to the tumor. The arterial redistribution was achieved by embolizing the internal thoracic artery (ITA) using a mixture of N-butyl cyanoacrylate (NBCA; B. Braun, Melsungen, Germany) and iodized oil (LPD) (Lipiodol Ultra-Fluide; Terumo, Tokyo, Japan) [13, 14]. Using this drug-delivery system, patients can be treated on an outpatient basis for extended periods of time. We believe that this new technique, named "redistributed subclavian arterial infusion chemotherapy" (RESAIC), is an epoch-making treatment method that, to the best of our knowledge, has not been reported previously. This study was an initial pilot study evaluating the effectiveness and safety of RESAIC.

Patients and Methods

Patients with ABC whose tumors were resistant to standard systemic chemotherapy or who were physically unable to tolerate systemic chemotherapy were the subjects of this study. In addition, patients >70 years of age with no previous treatment were also included. Eligibility criteria included histologically confirmed carcinoma of the breast, a life expectancy >2 months, World Health Organization performance status <3, adequate bone marrow reserve (white blood cell count >2500/ml, platelet count >50,000/ml), satisfactory renal and liver function (total bilirubin and creatinine <1.25 times the upper normal limits), and normal cardiac function by electrocardiogram (ECG). Any previous systemic chemotherapy except trastuzumab (Herceptin; Chugai, Japan) was discontinued for at least 4 weeks before protocol entry. Trastuzumab was continued to inhibit the development of distant metastases. Eleven patients were entered into this study between April 2006 and December 2007. All patients were female and had diagnosed stage IIIb or IV disease. A 52-year-old woman who had severe anemia (hemoglobin 5.6 g/dl) caused by bleeding from the primary tumor was entered because she was considered unable to tolerate standard systemic chemotherapy. All patients gave informed consent to participate in the trial. Table 1 shows demographics of the participating patients. The patients' ages ranged from 39 to 82 years (median of 61).

All patients were histologically diagnosed as having invasive ductal carcinoma, and one of the patients showed

Table 1 Patient's characteristics

Patient no.	Age	Tumor	Neoadjuvant or resistant	Stage	Distal metastasis	Symptom	Pathology	ER	PgR	Her2
1	58	Primary	Resistant	IV	Lung, liver	Pain	IDC/scirrhous carcinoma	+	+	1+
2	39	Primary	Resistant	IV	Lung, bone	Pain, ulcer, bleeding	IDC/papillo-tubular carcinoma	−	−	−
3	51	Recurrence	Resistant	IV	Lung, bone	Pain, ulcer, bleeding	IDC/scirrhous carcinoma	+	+	2+
4	52	Primary	Neoadjuvant	IIIb	–	Pain, bleeding, effusion	IDC	−	−	2+
5	72	Primary	Resistant	IIIb	–	Pain, ulcer, effusion	IDC	+	+	−
6	61	Recurrence	Resistant	IV	Liver	Pain, ulcer, effusion, arm edema	IDC/solid-tubular carcinoma	+	−	−
7	81	Primary	Neoadjuvant	IIIb	–	Pain, ulcer, effusion, arm edema	IDC	−	−	2+
8	78	Recurrence	Resistant	IIIb	–	Pain, erosion, induration	IDC (inflammatory breast cancer)	−	−	2+
9	70	Primary	Neoadjuvant	IV	Lung, bone	Pain, ulcer, bleeding, arm edema	IDC/scirrhous carcinoma	+	+	2+
10	82	Recurrence	Resistant	IV	Lung, liver	Pain, bleeding	IDC/solid-tubular carcinoma	+	−	−
11	52	Primary	Resistant	IV	Lung, liver, brain	Pain, bleeding, abscess formation	IDC/solid-tubular carcinoma	−	−	3+

IDC invasive ductal carcinoma

inflammatory breast cancer. Four patients had no distant metastasis. Three patients were previously untreated (neoadjuvant group) and eight were resistant to the previous systemic chemotherapy (resistant group). One patient had undergone mastectomy, and another patient had undergone radiotherapy. Overall tumor size ranged from 5.9 to 21.3 cm in diameter (median 10.5), from 10.5 to 13.9 cm (median 12.2) in the neoadjuvant group, and from 5.9 to 21.3 cm (median 6.7) in the resistant group. Tumor stages in the neoadjuvant group were IIIB in two patients and IV in one patient, and the stages in the resistant group were IIIB in two patients and IV in six patients.

Implantation of the CPS for RESAIC was performed by way of angiography with the patient under local anesthesia. First, embolization of the ITA was performed. In the first case, the ITA was embolized initially by way of a transfemoral approach. This was followed by implantation of the CPS by way of a brachial artery approach, and the port was placed in a subcutaneous pouch at the forearm (two-route method). In the other 10 patients, both embolization and implantation of the CPS were achieved with the ipsilateral brachial approach (one-route method). In the one-route method, the brachial artery was punctured at the level of the elbow joint, and a 4F 11-cm sheath was inserted. Subsequently, selective arteriograms of the subclavian artery and the internal thoracic artery were obtained with a 4F cobra-shaped catheter, a 4F pigtail catheter, or a hook-shaped catheter inserted through the sheath (Fig. 1A, B). Thereafter, embolization of the ITA was performed by a coaxial technique. To embolize the peripheral levels, a mixture of NBCA, which was diluted eight times with LPD (NBCA–LPD), was infused by way of a microcatheter advanced to approximately 3 cm distal to the tip of the parent catheter. To describing the procedure in more detail, the tip of the parent catheter was advanced up to the first corner of the ITA, and the tip of the microcatheter was further advanced to approximately 3 cm distal to the corner. The tip was placed in the straight-line part of the ITA. In eight cases, the proximal portion of the ITA was additionally embolized using one or two Tornado microcoils (Cook), 3–5 or 3–6 mm in diameter. After the embolization was confirmed with repeat arteriogram, implantation of the CPS was commenced (Fig. 1C, D). A long tapered Anthron-PU catheter (AP) with a distal shaft measuring 3.3F and 60 cm long and a proximal shaft measuring 5F and 40 cm long) was placed as an indwelling catheter with its tip positioned just distal to the ITA over a 0.025-inch guidewire. Before insertion, the length of the tapered 3.3F part of the AP was shortened to match the length from the puncture site to the placement site measured on the fluoroscopic monitor. The length ranged from 30 to 37 cm (median 32.4). After insertion of the AP, the distal end of the catheter was connected to a port (brachial type of Celsite port; Toray, Japan) and was implanted at the subcutaneous pouch approximately 5 cm distal to the puncture site in the forearm through the subcutaneous tunnel (Fig. 1E).

Treatment

To prevent perfusion to the arm, a sphygmomanometer cuff was used during injection of anticancer drugs. To evaluate drug distribution over the entire tumor, computed axial tomography arteriography (CTA) was performed while contrast material was infused by way of the implanted CPS. Drug distribution was evaluated in the most recent eight patients, except for one who had inflammatory breast cancer within the first treatment cycle of the protocol. CTA was started 30 seconds after injection of 30 ml contrast material, 50% diluted with saline, at a speed of 0.5 ml/s.

Bolus injections of anticancer agents were repeated weekly. Epirubicin (EP), 30 mg/body diluted with 20 ml distilled water, was injected during the implantation of the CPS as an initial treatment. From the second treatment onward, a treatment cycle consisted of cisplatin (10 mg/body) and 5-fluorouracil (5-FU) (750 mg/body) on days 1 and 8 and 15, and EP (20 mg/body) on days 22 of treatment. Both cisplatin and 5-FU were diluted with 20 ml normal saline, and EP was diluted with 20 ml distilled water. For two patients (patients no. 8 and 11), who had been treated with trastuzumab before undergoing our treatment, EP was excluded from the treatment protocol because of potential cardiac toxicity. In these patients, cisplatin (50 mg/body) and 5-FU (1000 mg/ body) were used at the initial injection instead of EP. Both drugs were diluted with normal saline, 100 and 20 ml, respectively. From the second treatment onward, the same doses of cisplatin and 5-FU were again injected. The drugs were injected at a speed of 1 ml/5 s for 60 seconds, and then the tourniquet was removed to reperfuse the arm for 30 seconds. This treatment cycle was repeated until all of the drugs were delivered for a particular session.

A decrease in leukocyte count <2,500 or platelet count <50,000 prompted us to interrupt the treatment until the counts increased. At leukocyte counts ranging from 2,500 to 3,000 or at platelet counts ranging from 50,000 to 100,000, the dosage of 5-FU was decreased to 500 mg/body. Cycles were repeated until sufficient regression was achieved. Blood counts and biochemistry tests were monitored weekly.

Treatment-related responses in the primary site tumors and regional lymph node metastases were evaluated by the change in the largest diameter of the lesion using the *Response Evaluation Criteria in Solid Tumors* (RECIST) manual [15]. Herein, measurable lesions are defined as tumors that can be measured accurately in at least one

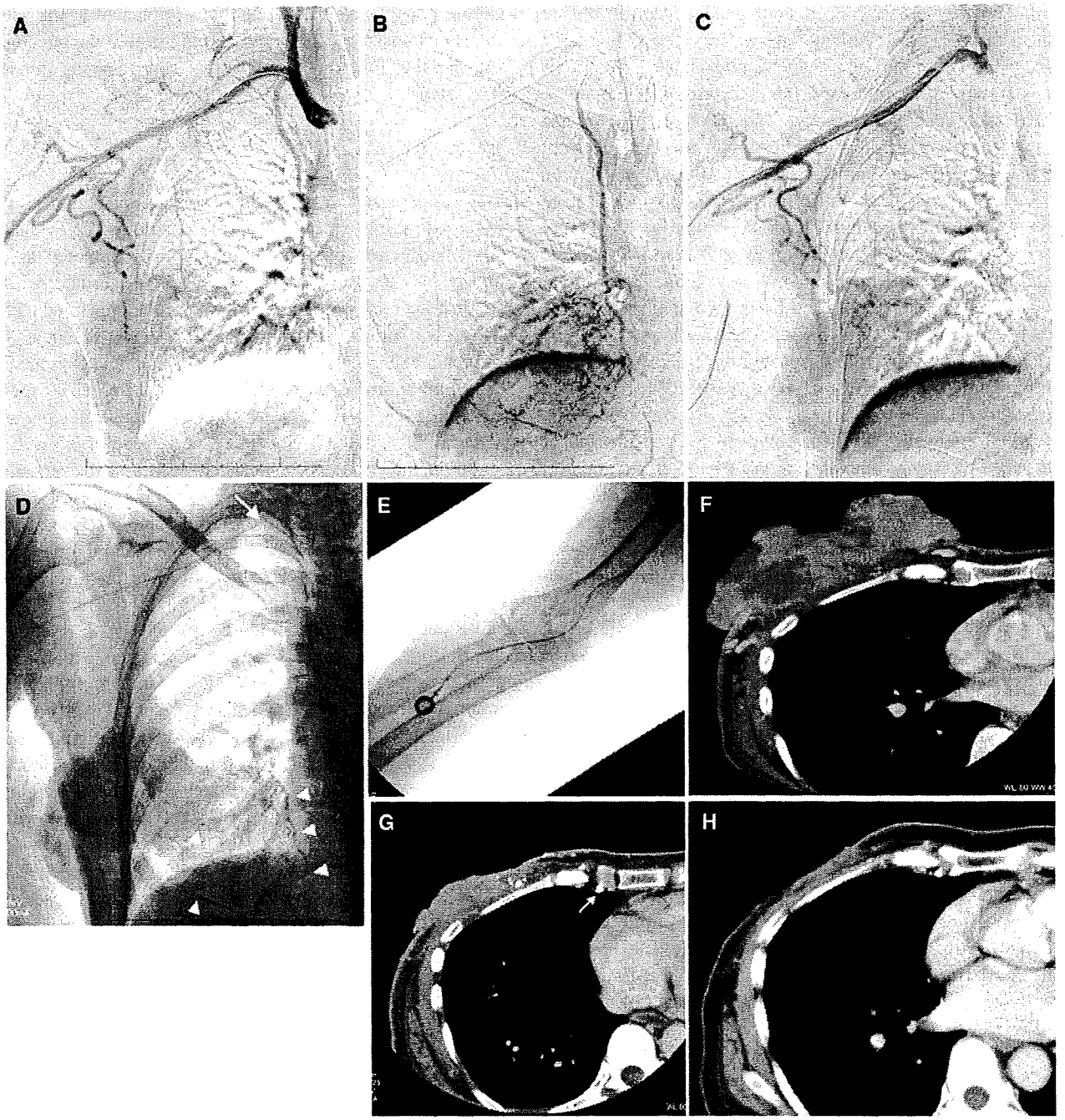

Fig. 1 (**A**) Digital subtraction angiography of subclavian artery by way of brachial approach in patient number 5 shows dilated internal and lateral thoracic arteries supplying advanced breast cancer. (**B**) A selective internal thoracic arteriogram was obtained using a 4F hook-shaped catheter. The medial part of the tumor is markedly opacified. (**C**) After embolization of the ITA using NBCA-LPD, a subclavian arteriogram was obtained by injection of contrast material by way of the indwelling catheter. The absence of opacification of the ITA was confirmed. (**D**) The scout film demonstrates the tip of the indwelling catheter (*white arrow*) placed just distal to the ITA as well as the accumulation of the infused NBCA-LPD (*white arrow heads*). (**E**) The distal end of the catheter was connected to the port and implanted at the subcutaneous pouch approximately 5 cm distal to the puncture site in the forearm through the subcutaneous tunnel. (**F**) Pretreatment CAT shows a huge tumor occupying the right-sided anterior chest wall. (**G**) CAT examination 1 month after starting RESAIC demonstrates a marked decrease in tumor size. Multiple high-density dots represent accumulation of NBCA-LPD in the ITA (*white arrow*) and its branches. (**H**) CAT examination 3 months later shows disappearance of the tumor. CR was diagnosed

dimension as being ≥10 mm and with a diameter that is more than twice the slice thickness (5 mm) by computed axial tomography (CAT) or magnetic resonance imaging (MRI). All measurable lesions, up to a maximum of 5, should be identified as target lesions, and these lesions should be selected in order of tumor size, starting with the largest.

Ten patients, except the one who had inflammatory breast cancer, were evaluated. Complete response (CR) was defined as disappearance of all target lesions. Partial response (PR) was defined as at least a 30% decrease in the sum of the largest diameters of the target lesions, using the baseline sum of the largest diameters as reference. Progressive disease (PD) was defined as at least a 20% increase in the sum of the largest diameters of the target lesions, using the baseline sum of the largest diameters as reference. Stable disease (SD) was defined as neither shrinkage sufficient to qualify for PR nor increase sufficient to qualify for PD. Not evaluable (NE) was defined when an evaluation by CT or MRI could not be done. CT and MRI scans were examined monthly. After the conclusion of RESAIC, clinical follow-up was carried out every 3 months. Procedure-related complications and treatment were scaled using version 3 of the National Cancer Institute's Common Terminology Criteria for Adverse Events [16].

Results

There were no serious procedure-related complications during CPS implantation nor were there any complications related to CPS during treatment. Two patients had grade 2 chest pain for a few days after embolization of ITA, but they had no visible dermal injury on the anterior chest wall, and the symptoms subsided without intervention. All patients were discharged within a few days after the procedure and continued infusions on an outpatient basis. The observation periods ranged from 90 to 553 days (average 310). Eight patients belonging to the resistant group required a dose-reduction of 5-FU because of decreased blood cell counts. Temporary grade-3 myelosuppression was seen in three patients belonging to the resistant group, requiring interruption of RESAIC for 2 weeks and administration of granulocyte colony-stimulating factor (G-CSF). The number of treatment cycles ranged from 3 to 10 (average 4.7), and the number of days when CPS was used ranged from 85 to 258 days (average 147.5).

The results of RESAIC are listed in Table 2. Nine of 10 (90%) patients showed PR or CR. The size of the tumor in one patient with inflammatory breast cancer could not be accurately measured on CT or MRI. In responder patients, at least some tumor reduction was observed within 1 treatment cycle. In three of four CR patients, resected specimens showed no residual cancer cells, and pathologic complete remission (PCR) was diagnosed in each of them. They have been alive and tumor free for 14, 9, and 2 months, respectively (Fig. 1F–H). The treatment of another CR patient in the resistant group with distant metastases was discontinued after 6 treatment cycles, and the patient was transferred to best supportive care after radiotherapy because of progression of her metastatic disease. The treatment of one patient with SD was discontinued after the patient had received 3 treatment cycles because of progression of lung metastasis. One patient (no. 3) with PR refused >3 treatment cycles because her preprocedural depression became worse. One patient who had inflammatory breast cancer underwent 5

Table 2 Treatment results

Patient no.	Treatment cycle	Beginning tumor size (cm)	Ending tumor size (cm)	Local response	Observation period (d)	Outcome
1	10	6.2	3.0	PR	553	Dead from metastasis
2	3	6.6	5.0	SD	351	Dead from metastasis
3	3	5.9	2.9	PR	141	Dead from metastasis
4	3	13.9	Scar	CR	539	Surgery → tumor free (14 mo)
5	5	6.8	Scar	CR	546	Surgery → tumor free (9 mo)
6	4	12.7	Scar	CR	373	Radiation, hepatic arterial chemotherapy
7	5	10.5	Scar	CR	252	Surgery → tumor free (2 mo)
8	5	–	–	NE	226	Observation
9	5	12.2	5.0	PR	192	Systemic chemotherapy
10	5	21.3	7.5	PR	144	Continuing SAIC
11	3	6.8	2.2	PR	90	Continuing SAIC

treatment cycles and had no exacerbation for 3 months after discontinuation of RESAIC. The treatment of one patient with PR (initial group) was interrupted after 5 treatment cycles because of bone metastasis progression. She was followed-up by systemic chemotherapy with aromatase inhibitors and capecitabine (Zeroda; Chugai, Japan). Currently, two patients have undergone RESAIC without complication. Entire tumors in the breast and axillary regions were remarkably enhanced on CTA in each of the eight patients examined. Even the recurrent tumor present in the medial portion of the chest wall after mastectomy was enhanced and responded to RESAIC (Fig. 2A–C). Symptoms-such as pain caused by skin ulceration, bleeding, foul odor, arm edema, or paresthesia-improved in all patients. The improvement of bleeding and pain was apparent a few days after the initial infusion, and arm edema improved as tumor size decreased.

All patients initially developed grade 1 skin hyperpigmentation in the infused areas ranging from the anterior chest wall to the back. Grade-1 alopecia occurred in two patients. The local symptoms improved, and RESAIC was continued on an outpatient basis without any significant complications in any patient.

Discussion

Currently, neoadjuvant systemic chemotherapy followed by local therapy is considered the standard treatment for controlling both local and inherent disseminated disease in patients with ABC [17]. However, an optimal chemotherapeutic regimen, local therapy, and optimal sequencing of those modalities have not been determined. Patients with ABC often suffer from symptoms, such as pain, bleeding, foul odor associated with infection, arm edema, or paresthesia. Therefore, preserving quality of life with local sterilization is given priority in such patients. AIC has often been applied as neoadjuvant chemotherapy for stage III tumors for the purpose of tumor downstaging [7, 8], as locoregional control of recurrent cancer [9], or as palliation [10]. In addition, it has been reported that AIC was feasible and effective in elderly patients [10]. However, selective and repeated infusion using the conventional procedure cause drug-induced damage of the infused arterial branches, and this promotes the development of a collateral arterial supply. Anatomically, the posterior intercostal and inferior epigastric arteries communicate to the anterior intercostal and superior epigastric arterial branches of the

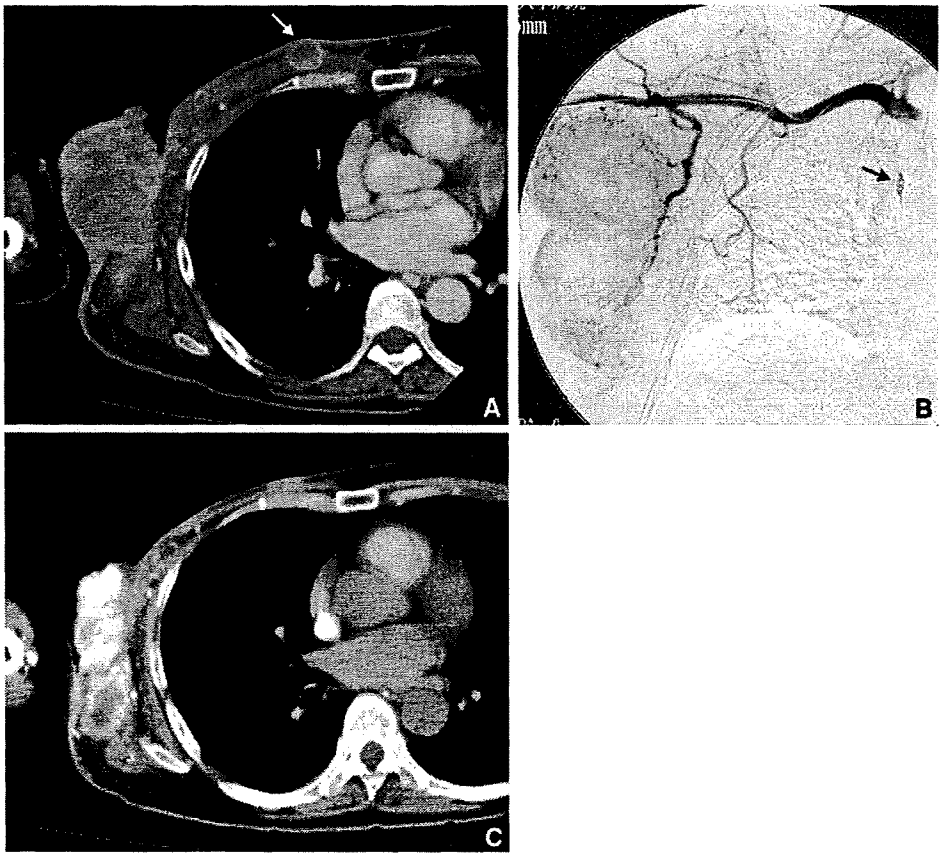

Fig. 2 (**A**) Pretreatment CTA of the patient number 6 shows a huge tumor metastasis in the right axillary region. Another metastatic tumor with ring enhancement (*white arrow*) is seen on the medial side of the anterior chest wall. (**B**) Pretreatment subclavian arteriogram by way of the implanted CPS demonstrates a huge tumor, which is mainly supplied by the lateral thoracic artery in the right axillary region. The *black arrow* represents embolized coils in the ITA. (**C**) CTA obtained by infusion of contrast material by way of the implanted CPS at the time of the third infusion chemotherapy demonstrates decreased sizes of both tumors and contrast enhancement of the tumors, which represents distribution of the infused drug

ITA. Therefore, it is reasonable to suppose that these arteries participate in the collateral arterial blood supply. Hence, the infused drug cannot be delivered to the entire tumor while AIC is being repeated. The number of possible repetitions of AIC is limited, and long-term local control cannot be expected. To deliver the infused drug efficiently to the entire tumor through a single implanted catheter–port system for an extended period of time, we developed RESAIC. The technical key point of RESAIC is the arterial redistribution of the subclavian artery achieved by ITA embolization using NBCA-LPD. This technique converges the multiple supplying arteries into a single subclavian arterial supply, thus inhibiting development of the collateral arteries. Drug distribution by CTA was satisfactory in all patients examined. The polymerization time of the mixture of NBCA diluted 8 times with LPD takes at least $\geq$10 seconds [18]. After which, the mixture was appropriate to embolize the peripheral levels of ITA in all patients. It is essential that NBCA-LPD is injected by way of a coaxial system relatively slowly, i.e., for approximately 10 seconds, to avoid problems associated with NBCA-LPD, such as migration or catheter fixation.

Many studies on AIC have reported that chemotherapy regimens, including anthracycline and 5-FU with or without other drugs, were efficient in downstaging ABC [3, 4, 6, 7, 10]. That is the reason why the regimens including EP and 5-FU, plus low-dose CDDP to modulate 5-FU, were designed.

Local chemoinfusion through a redistributed blood supply produced an overall response rate of 90%. Four patients had CR, and three of them showed PCCR. Two of the three patients who belonged to the neoadjuvant group had PCR, and the other patient had PR during treatment. Local symptoms improved, and RESAIC was continued on an outpatient basis in all patients without any significant complications. None of the patients had complications related to brachial arterial flow disturbance or cerebrovascular ischemia despite the long-term implantation of CPS. However, patients with a high risk of thromboembolism may need concomitant anticoagulation therapy. The drug must be infused slowly to prevent anticancer agents and potential thrombi from flowing out into the vertebral artery.

Our response rate was potentially higher than those reported in previous conventional AIC reports. Among them were a few reports on AIC using CPS [19, 20]. In these reports, the indwelling catheter was placed into the ITA or subclavian artery without arterial redistribution. Compared with our method, the number of infusion repeats were fewer, and the CR rate was lower (only 1 of 18 patients) [19].

In conclusion, RESAIC had a better response rate and no major complications compared with other studies despite the advanced stage of the cancer. Our results suggest that RESAIC is a reasonable and efficient locoregional treatment for ABC in elderly patients or in those who cannot physically tolerate chemotherapy, and it is available for patients with ABC who are resistant to systemic chemotherapy.

Because of our encouraging results, further larger-scale studies are needed in the near future to evaluate whether RESAIC is a treatment option that can improve local symptoms and prolong good quality of life in patients with ABC, even if RESAIC does not contribute to prolonged survival.

References

1. Haagensen CD (1986) Clinical classification of the stage of advancement of breast carcinoma. In: Haagensen CD (ed) Disease of the breast. W B Saunders, Philadelphia, pp 851–863
2. Japanese Breast Cancer Society (1989) The general rules for clinical and pathological recording of breast cancer. Jpn J Surg 19: 612–632
3. Murakami M, Kuroda Y, Nishimura S, Sano A, Okamoto Y, Taniguchi T et al (2001) Intraarterial infusion chemotherapy and radiotherapy with or without surgery for patients with locally advanced or recurrent breast cancer. Am J Clin Oncol 24:185–191
4. Kitagawa K, Yamakado K, Nakatsuka A, Tanaka N, Matsumura K, Takeda K et al (2002) Preoperative transcatheter arterial infusion chemotherapy for locally advanced breast cancer (stage IIIb) for down-staging and increase of resectability. Eur J Radiol 43:31–36
5. Fiorentini G, Tsetis D, Bernardeschi P, Varveris C, Rossi S, Kalogeraki A et al (2003) First-line intra-arterial chemotherapy (IAC) with epirubicin and mitoxantrone in locally advanced breast cancer. Anticancer Res 23:4339–4345
6. Koyama H, Wada T, Takahashi Y, Iwanaga T, Aoki Y (1975) Intra-arterial infusion chemotherapy as preoperative treatment of locally advanced breast cancer. Cancer 36:1603–1612
7. Stephens FO (1990) Intraarterial induction chemotherapy in locally advanced stage III breast cancer. Cancer 66:645–650
8. Görich J, Hasan I, Majdali R, Sittek H, Kunze V, Doma A, ET AL (1995) Previously treated, locally recurrent breast cancer: treatment with superselective intraarterial chemotherapy. Radiology 197: 199–203
9. Bufill JA, Grace WR, Neff R (1994) Intra-arterial chemotherapy for palliation of fungating breast cancer. A case report and review of the literature. Am J Clin Oncol 17:118–124
10. Pacetti P, Mambrini A, Paolucci R, Sanguinetti F, Palmieri B, Della Seta R, ET AL (2006) Intra-arterial chemotherapy: a safe treatment for elderly patients with locally advanced breast cancer. In Vivo 20:761–764
11. Seki H, Kimura M, Yoshimura M, Yamamoto S, Ozaki T, Sakai K (1998) Development of extrahepatic arterial blood supply to the liver during hepatic arterial infusion chemotherapy. Eur Radiol 8: 1613–1618
12. Ymagami T, Kato T, Tanaka O, Hirota T, Nishimura T (2005) Influence of extrahepatic arterial inflow into the posterior segment or caudate lobe of the liver on repeated hepatic arterial infusion chemotherapy. JVIR 16:457–463
13. Arai Y, Inaba Y, Takeuchi Y (1997) Interventional techniques for hepatic arterial infusion chemotherapy. In: Castaneda-Zuniga WR (ed) Interventional radiology, 2nd edn. Williams & Wilkins, Baltimore, pp 192–205
14. Yamagami T, Kato T, Iida S, Tanaka O, Nishimura T (2004) Value of transcatheter arterial embolization with coils and n-butyl cyanoacrylate for long-term hepatic arterial infusion chemotherapy. Radiology 230:792–802

15. Padhani AR, Ollivier L (2001) The RECIST (response evaluation criteria in solid tumors) criteria: implications for diagnostic radiologists. Br J Radiol 74:983–986
16. Trotti A, Colevas AD, Setser A, Rusch V, Jaques D, Budach V et al (2003) CTCAE v3.0: development of a comprehensive grading system for the adverse effects of cancer treatment. Semin Radiat Oncol 13:176–181
17. Wang HC, Lo SS (1996) Future prospects of neoadjuvant chemotherapy in treatment of primary breast cancer. Semin Surg Oncol 12:59–66
18. Stoesslein F, Ditscherlein G, Romaniuk PA (1982) Experimental studies on new liquid embolization mixtures (histoacryllipiodol, histoacryl-panthopaque). Cardiovasc Intervent Radiol 5:264–267
19. Cakmakli S, Ersöz S, Tug T, Karaayvaz M, Akgül H (1997) Intra-arterial infusion chemotherapy in the treatment of locally advanced breast cancer. Acta Oncol 36:489–492
20. Grosso M, Zanon C, Mancini A, Garruso M, Gazzera C, Anselmetti GC et al (2000) Percutaneous implantation of a catheter with subcutaneous reservoir for intraarterial regional chemotherapy: technique and preliminary results. Cardiovasc Intervent Radiol 23: 202–210

Immunoglobulin G4–related Lung Disease: CT Findings with Pathologic Correlations[1]

Dai Inoue, MD
Yoh Zen, MD
Hitoshi Abo, MD
Toshifumi Gabata, MD
Hiroshi Demachi, MD
Takeshi Kobayashi, MD
Jyun Yoshikawa, MD
Shiro Miyayama, MD
Masahide Yasui, MD
Yasuni Nakanuma, MD
Osamu Matsui, MD

Purpose: To retrospectively analyze radiologic findings of immunoglobulin G4 (IgG4)-related lung disease as correlated with pathologic specimens.

Materials and Methods: This study was approved by the institutional review board, and all patients had consented to the use of their medical records for the purpose of research. This study included 13 patients with IgG4-related lung disease (nine men and four women; age range, 43–76 years). Computed tomographic (CT) findings were retrospectively analyzed with regard to the characteristics, shape, and distribution of the radiologic findings and were correlated with surgically resected or biopsy lung specimens in seven patients. Statistical analysis was not used in this study.

Results: On the basis of the predominant radiologic abnormality, IgG4-related lung disease could be categorized into four major subtypes: solid nodular type having a solitary nodular lesion that included a mass (four patients); round-shaped ground-glass opacity (GGO) type characterized by multiple round-shaped GGOs (two patients); alveolar interstitial type showing honeycombing, bronchiectasis, and diffuse GGO (two patients); and bronchovascular type showing thickening of bronchovascular bundles and interlobular septa (five patients). Pathologically, solitary nodular lesions consisted of diffuse lymphoplasmacytic infiltration with fibrosis. Thickened bronchovascular bundles or interlobular septa and GGO on CT images pathologically corresponded to lymphoplasmacytic infiltration and fibrosis in peribronchiolar or interlobular interstitium and alveolar interstitium, respectively. The radiologic findings of honeycombing corresponded to disrupted alveolar structures and dilated peripleural air spaces.

Conclusion: IgG4-related lung disease manifested as four major categories of CT features. Pathologically, these features corresponded to IgG4-related sclerosing inflammation along the intrapulmonary connective tissue.

[1] From the Departments of Radiology (D.I., T.G., O.M.), Respiratory Medicine (M.Y.), and Human Pathology (Y.N.), Kanazawa University Graduate School of Medical Science, 13-1 Takaramachi, Kanazawa 920-8641, Japan; Division of Pathology, Kanazawa University Hospital, Kanazawa, Japan (Y.Z.); Department of Radiology, Toyama Prefectural Central Hospital, Toyama, Japan (H.A., H.D.); Department of Radiology, Ishikawa Prefectural Central Hospital, Kanazawa, Japan (T.K.); Department of Radiology, Fukui Prefectural Hospital, Fukui, Japan (J.Y.); and Department of Radiology, Fukuiken Saiseikai Hospital, Fukui, Japan (S.M.). Received June 2, 2008; revision requested July 15; revision received September 25; accepted October 15; final version accepted October 26. **Address correspondence to** D.I. (e-mail: *d-inoue@lake.ocn.ne.jp*).

Recently, increasing attention has been drawn to immunoglobulin G4 (IgG4)-related diseases (1). In 2001, Hamano et al (2) reported that patients with sclerosing pancreatitis, also called autoimmune pancreatitis, had high serum IgG4 concentrations. Subsequently, IgG4-related lesions similar to those of autoimmune pancreatitis have been identified in other organs such as the bile duct (sclerosing cholangitis) (3), salivary gland (chronic sclerosing sialadenitis or Küttner tumor) (4), lacrimal gland (chronic sclerosing dacryoadenitis) (5), liver (inflammatory pseudotumor) (3), retroperitoneum (retroperitoneal fibrosis) (6), kidney (tubulointerstitial nephritis), and the aorta (inflammatory aneurysm) (7).

The radiologic features of IgG4-related diseases have been reported, especially those of the pancreatic lesion (autoimmune pancreatitis) (8). More recently, Takahashi et al (9) reported radiologic characteristics of IgG4-related renal lesions (9), all of which were associated with autoimmune pancreatitis. There have been several reports about IgG4-related lung diseases, although most of them were single case reports (10–12). Subsequently, we also reported that some pulmonary inflammatory pseudotumors (plasma cell granulomas) are pathologically inflammatory lesions containing numerous IgG4-positive plasma cells (13). We concluded that pulmonary inflammatory pseudotumor could be one kind of IgG4-related lung disease. It is now recognized that IgG4-related lung disease can manifest as inflammatory pseudotumor or interstitial inflammation (14,15). However, the disease spectrum of IgG4-related lung disease has yet to be fully revealed. The purpose of this study was to retrospectively analyze radiologic findings of IgG4-related lung disease as correlated with pathologic specimens.

Advances in Knowledge

- Immunoglobulin G4 (IgG4)-related disease shows various types of pulmonary manifestations.
- IgG4-related lung disease can be categorized into four types on the basis of the predominant CT findings: solid nodular, round-shaped ground glass opacity, alveolar interstitial, and bronchovascular.
- IgG4-related lung disease can be considered a IgG4-related sclerosing inflammation along the entire intrapulmonary connective tissue.

Materials and Methods

Case Selection

This study was approved by our institutional review board. All patients had consented to the use of their medical records for the purpose of research. A total of 13 cases were selected from the pathology files of our hospital and related institutions from the period between September 1998 and November 2007. Clinical records were available for all patients and were reviewed for presenting clinical symptoms and laboratory data. Patients' age, sex, clinical symptoms, and laboratory data, including serum IgG4 concentration, are listed in Table 1. Of the 13 patients (nine men [mean age, 59 years; range, 43–75 years] and four women [mean age, 70 years; range, 59–76 years]; mean age, 62 years; range, 43–76 years), four (cases 1–4) underwent surgical resection of the pulmonary lesions because of a suspicion of lung cancer (cases 1–3, partial resection; case 4, right pneumonectomy). Three patients (cases 6, 7, 10) underwent surgical biopsy of the lung by means of video-assisted thoracic surgery. In the remaining six patients, IgG4-related disease was diagnosed by means of biopsy of extrapulmonary organs such as the kidney (cases 8 and 11), prostate (case 9), cervical lymph node (case 12), periaortic soft tissue (case 5), or ampulla of Vater (case 13). Pulmonary lesions in those six patients were not pathologically examined, but radiologic abnormalities showed similar characteristics to those in other patients who were proved to have IgG4-related lung disease at pathologic examination of lung specimens. Therefore, we included these six patients in this study. Extrapulmonary IgG4-related diseases were identified in eight patients: autoimmune pancreatitis (cases 4, 11, 13), periaortitis (cases 5, 12), interstitial nephritis (cases 8, 11, 12), chronic sclerosing sialadenitis (cases 8, 10, 13), and prostatitis (case 9).

Implication for Patient Care

- Knowledge of the CT findings and their pathologic background is inevitable to correctly diagnose IgG4-related lung disease and to avoid unnecessary surgical procedure or other medical treatment in a patient with a diagnosis of malignant tumor or other inflammatory diseases.

Radiologic Examination

Computed tomographic (CT) images were available for all patients and were reviewed. Single-, eight-, 16-, and 64-detector row CT examinations were performed in four, two, three, and four patients, respectively. Because of the multi-institutional retrospective nature of this study, the scanning protocols were not considered. In this study, information about all protocols was not available in the cases from other institutions. Information about the section thickness, tube voltage, and tube current was available for all patients and was noted, but information about pitch was not available. Initially, chest CT scans were obtained throughout the chest with a section thickness of 2.5 mm in one patient, 5 mm in seven patients, 7.5 mm in two patients, and 10 mm in three pa-

Published online before print
10.1148/radiol.2511080965

Radiology 2009; 251:260–270

Abbreviations:
GGO = ground-glass opacity
IgG = immunoglobulin G

Author contributions:
Guarantors of integrity of entire study, D.I., H.A., T.G., M.Y., O.M.; study concepts/study design or data acquisition or data analysis/interpretation, all authors; manuscript drafting or manuscript revision for important intellectual content, all authors; approval of final version of submitted manuscript, all authors; literature research, D.I., H.A., S.M.; clinical studies, all authors; experimental studies, H.A.; statistical analysis, H.A.; and manuscript editing, D.I., Y.Z., H.A., T.G., O.M.

Authors stated no financial relationship to disclose.

tients (120 kVp and 180 mAs for single-detector row scanners, 135–140 kVp and 180–270 mAs for multi-detector row scanners). Subsequently, thin-section CT images with 1.0–2.0-mm section thickness with or without section interval were obtained for all patients.

Image Analysis

All chest CT images were reviewed by two radiologists (D.I. and H.A., with 6 and 15 years of thoracic CT imaging experience, respectively), and decisions were reached by consensus. The CT images were evaluated for the presence and distribution of mass, large nodules, small nodules, ground-glass opacity (GGO), thickening of bronchovascular bundles, thickening of interlobular septa, bronchiectasia, honeycombing, cysts, enlarged lymph node, and pleural effusion. These CT findings were selected for the analysis according to the preliminary review of the CT images and previous case reports (10–12). Mass was defined as a solid lesion larger than 3.0 cm in diameter. Solid nodules were defined as large when they were equal to or larger than 1.0 cm and as small when smaller than 1.0 cm. GGO was seen as a hazy increase in attenuation. Underlying vascular structures were observed in GGO, but not in any of the mass and nodular lesions. Lymph nodes larger than 1.0 cm in the short axis were interpreted as enlarged. The number of lesions was also analyzed as follows: solitary, two to five, and multiple (> five) for mass and nodular lesions. GGO was classified into two types: round shaped and diffuse. Round-shaped GGO was well defined and had round-shaped border, whereas diffuse GGO was poorly defined and showed patchy or irregular shape.

In seven patients (cases 1–4, 6, 7, 10) who underwent a surgical procedure for the lung lesions, we examined

Table 1

Clinical Features and Laboratory Data

Case No./ Age (y)/Sex	Clinical Symptom	ANA (titer)	IgG* (mg/dL)	IgG4† (mg/dL)	IgG4/IgG Ratio (%)
1/51/M	Chest pain	×80	2250	NA	NA
2/72/F	None	NA	1560	NA	NA
3/76/F	Cough	×80	2150	NA	NA
4/70/M	Cough	<20	2150	462	21
5/55/M	Low-grade fever	<20	2300	392	17
6/43/M	None	NA	2530	222	9
7/59/M	Cough, dyspnea on exertion	×640	2480	325	13
8/75/M	Fever	×80	2600	1010	39
9/59/M	Cough	NA	2170	1130	52
10/71/F	Cough, low-grade fever	×60	5180	NA	NA
11/59/F	Cough	×40	2544	926	36
12/71/M	Cough, low-grade fever, dyspnea on exertion	<20	4970	NA	NA
13/48/M	None	<20	2210	1550	70

Note.—ANA = antinuclear antibodies, IgG = immunoglobulin G, NA = not analyzed.

* To convert to Système International (SI) units (grams per liter), multiply by 0.01. Normal range, less than 1600 mg/dL.

† To convert to SI units (grams per liter), multiply by 0.01. Normal range, less than 110 mg/dL.

Table 2

Radiologic Findings in 13 Cases of IgG4-related Lung Disease

Case No.	Mass	Large Nodule (>1.0 cm)	Small Nodule (≤1.0 cm)	GGO	Thickening of Bronchovascular Bundle	Thickening of Interlobular Septa	Bronchiectasia	Honeycombing	Cyst	Enlarged Lymph Node
1	No	Solitary (2.0 cm)	No	Yes	Yes	No	No	No	No	No
2	No	Solitary (1.8 cm)	No	Yes	Yes	No	Yes	No	No	No
3	No	Solitary (1.2 cm)	No	Yes	No	No	No	No	No	No
4	Solitary (6.5 cm)	No	No	Yes	Yes	Yes	No	No	No	Yes
5	No	No	No	Yes	No	No	Yes	No	No	No
6	No	No	No	Yes	No	No	No	No	No	No
7	No	No	No	Yes	Yes	Yes	Yes	Yes	No	Yes
8	No	No	No	Yes	Yes	Yes	Yes	Yes	No	Yes
9	No	No	No	Yes	Yes	Yes	Yes	No	No	Yes
10	No	No	Multiple	Yes	Yes	Yes	Yes	No	Yes	Yes
11	No	No	Multiple	Yes	Yes	Yes	No	No	No	No
12	No	No	No	Yes	Yes	Yes	Yes	No	No	Yes
13	No	No	No	No	Yes	Yes	No	No	No	No
Total	1 (8)	3 (23)	2 (16)	12 (92)	9 (69)	8 (62)	7 (54)	2 (15)	1 (8)	6 (46)

Note.—Unless otherwise indicated, data in parentheses are percentages.

each radiologic finding as correlated with the pathologic specimen. Correlation between radiologic and pathologic findings was examined by two the radiologists and one surgical pathologist (Y.Z., with 10 years of experience), and decisions were reached by consensus.

Pathologic Examination

Pathologic diagnoses of IgG4-related disease were made from specimens obtained from the lung (surgery, cases 1–5, 7, 10), kidney (needle biopsy, cases 8 and 11), periaortic soft tissue (needle biopsy, case 6), prostate (needle biopsy, case 9), cervical lymph node (excisional biopsy, case 12), and ampulla of Vater (biopsy, case 13). The original resection or biopsy specimens were available for all patients and were reviewed by the surgical pathologist. The procedure for diagnosing IgG4-related disease is described next.

Diagnosis of IgG4-related disease.—Formalin-fixed and paraffin-embedded specimens were prepared and used for histopathologic and immunohistochemical examination. Four-micron sections were cut for hematoxylin-eosin, elastica-van Gieson, and immunohistochemical stainings. IgG4-related disease was diagnosed on the basis of pathologic features such as diffuse lymphoplasmacytic infiltration, irregular fibrosis, occasional eosinophilic infiltration, and obliterative vasculitis.

Immunohistochemistry.—Immunostaining of IgG, IgG4, κ chain, and λ chain was performed with an autostainer (HX System Benchmark; Ventana Medical Systems, Tucson, Ariz) according to the manufacturer's instructions. Primary antibodies used were a rabbit polyclonal antibody against human IgG (Dako Cytomation, Glostrup, Denmark), a mouse monoclonal antibody for human IgG4 (Zymed Laboratory, San Francisco, Calif), a mouse monoclonal antibody for human κ chain (Medical & Biological Laboratories, Nagoya, Japan), and a mouse monoclonal antibody for human λ chain (Medical & Biological Laboratories). Sections were pretreated with proteinase (IgG and IgG4) and a heated plate (κ and λ chains) (16).

Pathologic Features of IgG4-related Disease

Pulmonary nodular lesions in cases 1–4 pathologically consisted of diffuse lymphoplasmacytic infiltration, fibrosis, and frequent eosinophilic infiltration (Fig 1a, 1b). Obliterative phlebitis and angitis were observed in all of those cases (Fig 1c, 1d). Specimens from the lung in cases 6 and 7 showed interstitial thickening with lymphoplasmacytic infiltration. Eosinophils and lymph follicles were easily identified. Severe lymphoplasmacytic infiltration was also identified in interlobular septa or peribronchiolar interstitium.

Figure 1

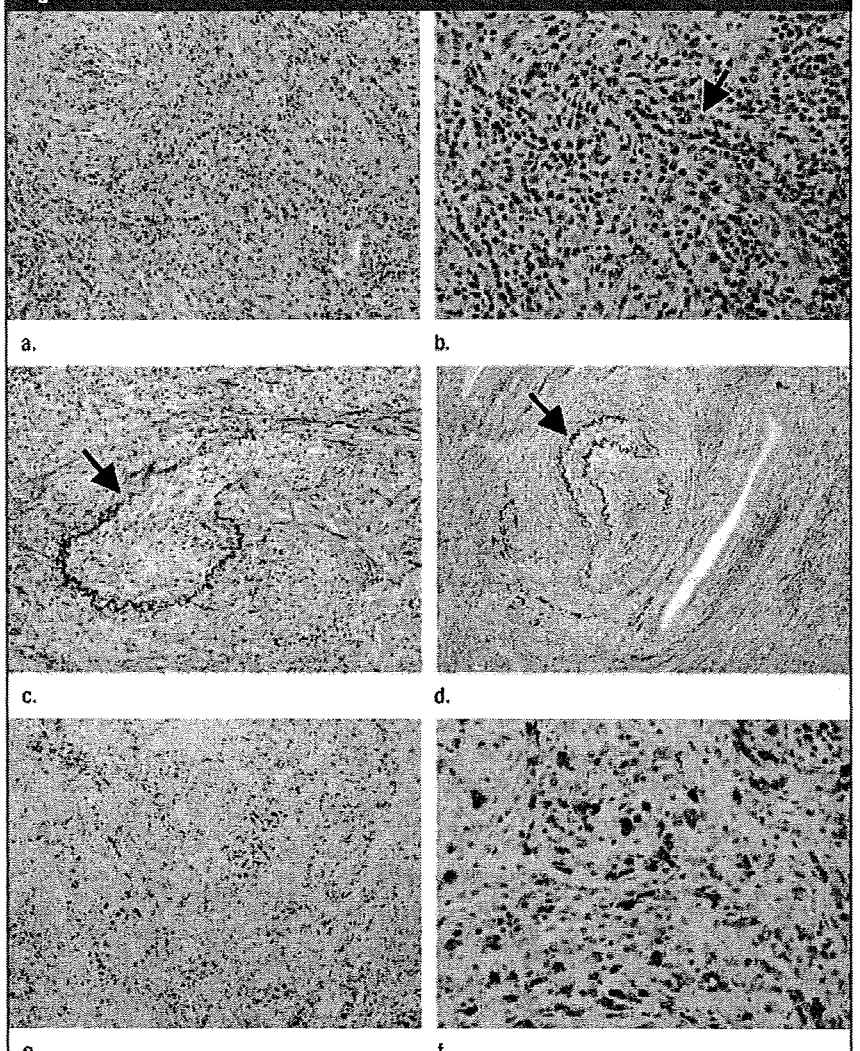

Figure 1: Histologic findings of IgG4-related lung disease. **(a)** Solid nodular lesions show diffuse lymphoplasmacytic infiltration and fibrosis. (Hematoxylin-eosin stain, original magnification, ×200.) **(b)** Inflammatory cells mainly consist of lymphocytes and plasma cells; some eosinophils are also observed (arrow). (Hematoxylin-eosin stain, original magnification, ×400.) **(c)** Obliterative phlebitis (arrow). (Elastica-van Gieson stain, original magnification, ×200.) **(d)** Arterial branch occluded by sclerosing inflammation (arrow). (Elastica-van Gieson stain, original magnification, ×100.) **(e, f)** Immunostaining of IgG4 reveals numerous IgG4-positive plasma cells. (Magnification in **e**, ×100; and in **f**, ×400.)

Biopsy of the kidney (cases 8, 11), periaortic soft tissue (case 6), prostate (case 9), and ampulla of Vater (case 13) revealed diffuse lymphoplasmacytic infiltration with occasional eosinophils. Renal tubules, prostatic glands, and duodenal glands were atrophied. Obliterative phlebitis could not be identified in those samples probably because of the small size of the specimens. Lymph nodes in case 12 histologically showed expansion of the interfollicular area, in which many plasma cells were identified. Lymph follicles were also hyperplasic. This lesion was originally diagnosed as Castleman-like lymphadenopathy. After immunostaining of IgG4, the pathologic diagnosis was corrected to IgG4-related lymphadenopathy.

Immunostaining of IgG4 revealed abundant IgG4-positive plasma cells in all specimens. IgG4-positive plasma cells were diffusely distributed within the lesions (Fig 1e, 1f). In pulmonary lesions, IgG4-positive plasma cells were observed in inflamed areas such as nodular lesions, alveolar interstitium, interlobular septa, and peribronchial or peribronchiolar interstitium. Numerous IgG4-positive plasma cells were identified in all cases with immunostaining (79–335 cells per high-power field). Ratios of IgG4/IgG-positive plasma cells were more than 30% in all cases. Immunostaining of κ and λ chains showed polyclonal B cells and plasma cells. No atypical cells suggestive of a neoplastic process could be identified in any lesion.

Figure 2

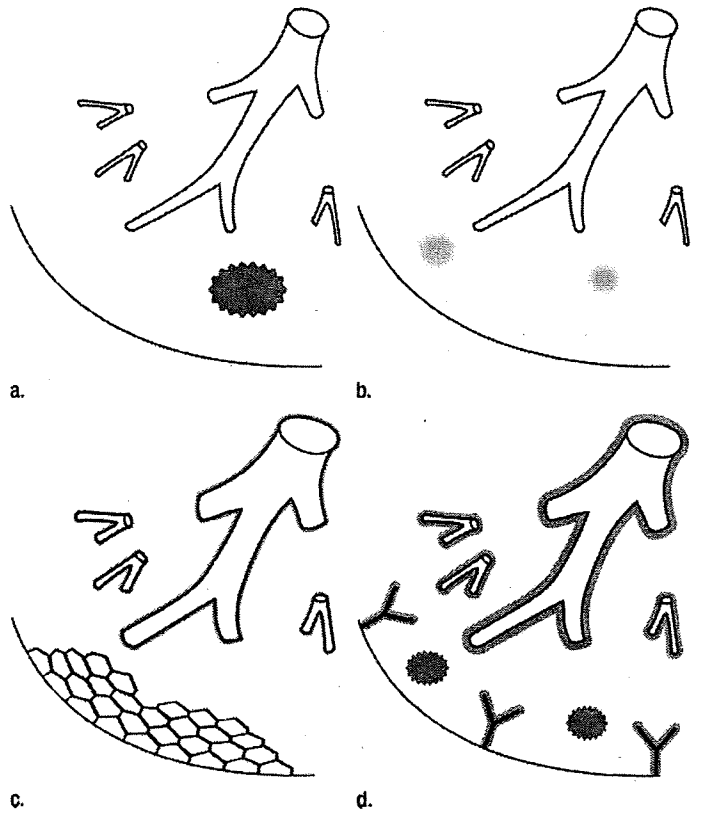

Figure 2: Schematic of four types of IgG4-related lung disease: **(a)** solid nodular, **(b)** round-shaped GGO, **(c)** alveolar interstitial, and **(d)** bronchovascular.

Results

Radiologic Findings

As shown in Table 2, 10 radiologic findings were identified. These findings consisted of a mass, large nodules, small nodules, GGO, thickening of bronchovascular bundles, thickening of interlobular septa, bronchiectasia, honeycombing, cysts, and lymph node enlargement. Pleural effusion was not seen in any of the cases. Mass and large nodules were identified as solitary lesions, to the contrary, small nodules were seen as multiple lesions. Two patients (cases 5, 6) had round-shaped GGO in multiple lobes. Diffuse GGO was identified in 10

Table 3

Type, Location, and Initial Radiologic Diagnoses in 13 Cases of IgG4-related Lung Disease

Case No.	Type of Radiologic Finding	Location	Initial Diagnosis
1	Solid nodular	Left lower lobe	Lung cancer
2	Solid nodular	Right lower lobe	Lung cancer
3	Solid nodular	Left upper lobe	Lung cancer
4	Solid nodular	Right upper lobe and hilum	Lung cancer
5	Round-shaped GGO	Right upper and lower	Lung cancer (bronchioloalveolar carcinoma)
6	Round-shaped GGO	All lobes	Lung cancer (bronchioloalveolar carcinoma)
7	Alveolar interstitial	All lobes	Nonspecific interstitial pneumonia
8	Alveolar interstitial	All lobes	Nonspecific interstitial pneumonia
9	Bronchovascular	All lobes	Lymphoproliferative disorder or sarcoidosis
10	Bronchovascular	All lobes	Lymphoproliferative disorder or sarcoidosis
11	Bronchovascular	All lobes	Lymphoproliferative disorder or sarcoidosis
12	Bronchovascular	All lobes	Lymphoproliferative disorder or sarcoidosis
13	Bronchovascular	All lobes	Lymphoproliferative disorder or sarcoidosis

patients (cases 1–4, 7–12) in multiple lobes. One patient (case 5) had only round-shaped GGO, whereas the remaining 12 patients had multiple radiologic abnormalities (Table 2). On the basis of the predominant radiologic features in the 13 patients, they could be classified into four types (Fig 2): solid nodular, round-shaped GGO, alveolar interstitial, and bronchovascular (Table 3).

The first is a solid nodular type. This type (cases 1–4) was characterized by the presence of a solitary solid lesion larger than 1.0 cm that included a mass.

Figure 3

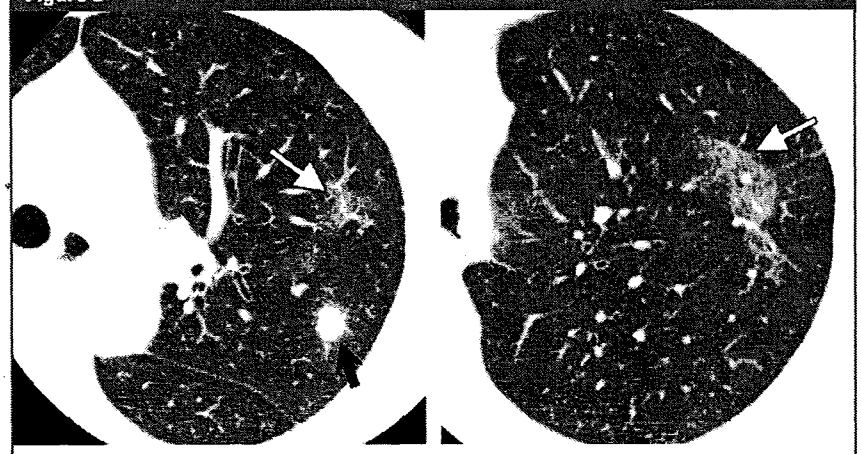

a. b.

Figure 3: (a, b) Thin-section CT scans of left lung in a 76-year-old woman (case 3) with IgG4-related lung disease demonstrate a solid nodule in the left upper lobe (black arrow). This nodule is accompanied by perinodular spiculation. Diffuse GGO is also shown in the left upper lobe separated by a solid nodule (white arrows).

Figure 4

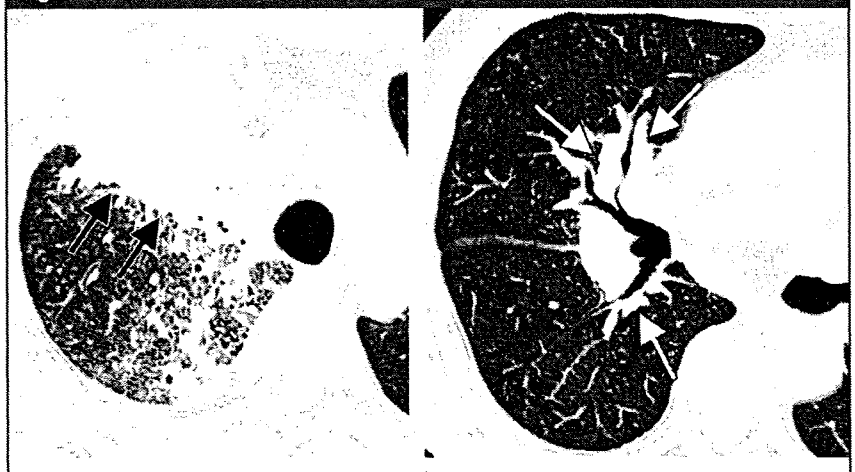

a. b.

Figure 4: (a, b) Thin-section CT scans of right lung in a 70-year-old man (case 4) with IgG4-related lung disease. (a) Image reveals mass in the right upper lobe (arrows); diffuse GGO is found around the mass. (b) Thickening of bronchovascular bundles in the right hilum (arrows).

Nodules in cases 1–3 were subtle with focal spiculated appearance (Fig 3). In contrast, case 4 showed a mass widely extending to the right upper lobe, and this lesion also involved a central bronchus causing thickening of peribronchial interstitium (Fig 4). All cases of the solid nodular type were initially thought to be primary lung cancer (Table 3). Notably, case 4 was thought to be hilar lung cancer with obstructive pneumonia. Three patients (cases 1–3) underwent partial resection, and nodular lesions were pathologically diagnosed as inflammatory nodules at frozen-section diagnosis. One patient (case 4) underwent right pneumonectomy, and the pathologic diagnosis of inflammatory pseudotumor was made.

The next is a round-shaped GGO type (case 5, 6), which was radiologically characterized by multiple round-shaped GGOs (Fig 5). The bronchus involved in GGO was slightly dilated in case 5. In these two cases, GGO was identified in multiple lobes; however, each lesion was round shaped and well defined. The radiologic findings of this type resembled those of bronchioloalveolar carcinoma (Table 3).

The third is the alveolar interstitial type (cases 7, 8), which is radiologically characterized by diffuse GGO, bronchiectasia, and honeycombing (Fig 6). The patients were initially suspected of having nonspecific interstitial pneumonia on the basis of radiologic findings (Table 3).

The last is the bronchovascular type (cases 9–13). Radiologic finding of this type is thickening of bronchovascular bundles and interlobular septa (Fig 7). Of five patients with this type, two (cases 10 and 11) had multiple small nodules, most of which were located in the centrilobular area (Fig 8). Three patients (cases 9, 10, 12) also had lymph node swelling in the hilum and mediastinum. Thin-walled cysts were identified in only one patient (case 10). Sarcoidosis or lymphoproliferative disorders such as multicentric Castleman disease were radiologically suspected in those cases (Table 3).

Radiologic abnormalities were seen in all lung zones in cases of alveolar

Figure 5

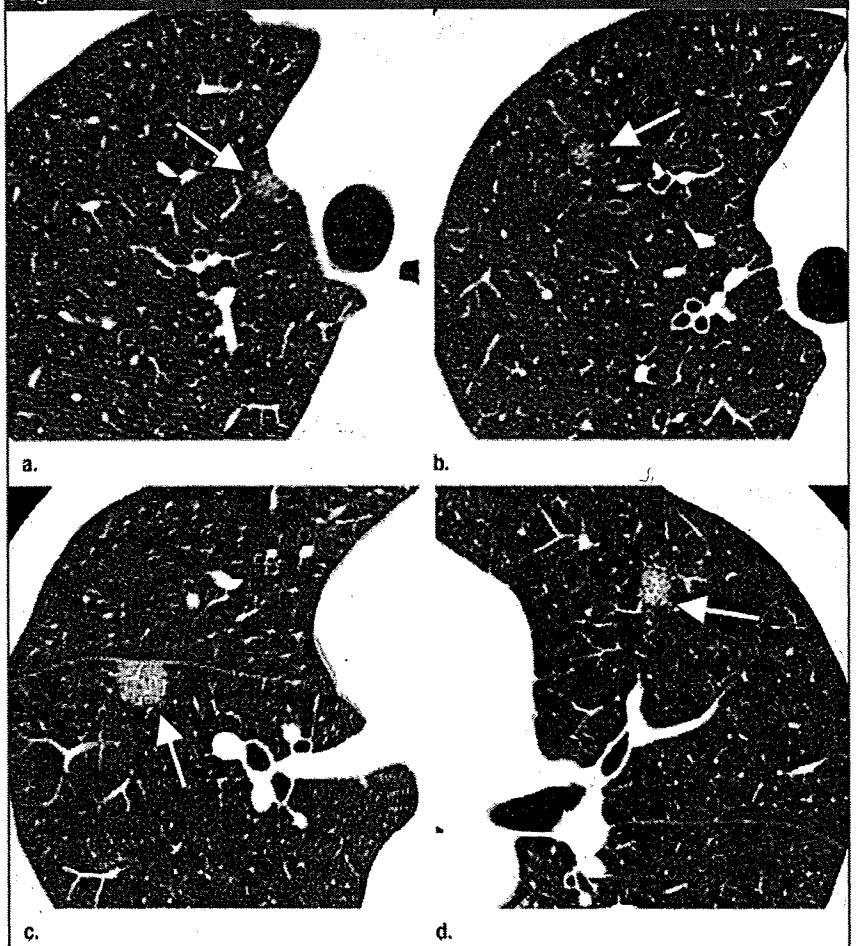

Figure 5: **(a–d)** Thin-section CT scans in a 43-year-old man (case 6) with IgG4-related lung disease. Multiple GGOs are shown in both lungs. Each lesion is well defined and round shaped (arrow).

interstitial type or bronchovascular type, whereas they were identified in only one lobe in solid nodular type.

Radiologic and Pathologic Correlations

We examined radiologic and pathologic correlations in seven patients, all of whom underwent surgical resection or biopsy of the lung. Large nodules pathologically consisted of diffuse lymphoplasmacytic infiltration with fibrosis (Fig 1a). Alveolar structures could not be identified within nodules. Sclerosing inflammation extended along the interlobular septa and thickened alveolar wall at the edge of solid lesions (Fig 9a). Those findings corresponded to radiologic findings of spiculated appearance around solid lesions. Small nodular lesions histologically corresponded to sclerosing inflammation in the peribronchiolar area (Fig 9b). Lymph follicles were associated with sclerosing inflammation in some cases.

The radiologic finding of GGO was histologically characterized by inflammatory cell infiltration in a slightly thickened alveolar interstitium (Fig 9c). The distribution of inflammation and fibrosis was relatively even. These pathologic features resembled nonspecific interstitial pneumonia pattern. Several lymph follicles were also associated with sclerosing inflammation. In the advanced lesions, alveolar structures were thickened and disrupted and peripleural air spaces were cystically dilated (Fig 9d). These histologic findings corresponded to the radiologic finding of honeycombing. Bronchi or bronchioles involved in the lesions were also slightly dilated on histologic specimens.

Thickened bronchovascular bundles or interlobular septa at CT histologically showed lymphoplasmacytic infiltration with stromal fibrosis (Fig 9e, 9f). Peribronchial glands were involved in the inflammation. Inflammatory processes extended along peribronchiolar interstitium. Bronchial inflammation was confined to bronchial wall, while the bronchial epithelium was preserved.

Discussion

On the basis of our results, four major types of IgG4-related lung disease could be defined: solid nodular, round-shaped GGO, alveolar interstitial, and bronchovascular. Solid nodular and round-shaped GGO-type lesions can mimic primary lung cancer including bronchioloalveolar carcinoma. Indeed, primary lung cancer was initially suspected in these cases on the basis of CT findings. The differential diagnosis of bronchovascular-type lesions includes lymphoproliferative disorders such as multicentric Castleman disease, sarcoidosis, and lymphangitis carcinomatosa. Alveolar interstitial-type lesions radiologically resemble nonspecific interstitial pneumonia. That is, IgG4-related lung diseases should be differentiated from a variety of lung diseases, including neoplastic and non-neoplastic lesions, and differential diagnoses of each case depend on the radiologic types of IgG4-related lung disease. IgG4-related disease seen in pancreas (autoimmune pancreatitis) or kidney shows a variety of imaging features despite the same pathologic change (8,9). Therefore, we speculate that the four types of IgG4-related lung disease did not represent different disorders but were part of the morphological spectrum of a single pathologic condition like other organs affected by IgG4-related disease. We examined 13 cases of IgG4-related lung disease and detected four types of radiologic manifestations of IgG4-related lung disease; however, more varieties of radiologic manifestation might be found by examining more large study groups.